

# Deep Reinforcement Learning of Cell Movement in the Early Stage of *C. elegans* Embryogenesis

Zi Wang<sup>1</sup>, Dali Wang<sup>1,3,\*</sup>, Chengcheng Li<sup>1</sup>, Yichi Xu<sup>2</sup>, Husheng Li<sup>1</sup> and Zhirong Bao<sup>2</sup>

**Abstract**—Cell movement in the early phase of *C. elegans* development is regulated by a highly complex process in which a set of rules and connections are formulated at distinct scales. Previous efforts have demonstrated that agent-based, multi-scale modeling systems can integrate physical and biological rules and provide new avenues to study developmental systems. However, the application of these systems to model cell movement is still challenging and requires a comprehensive understanding of regulation networks at the right scales. Recent developments in deep learning and reinforcement learning provide an unprecedented opportunity to explore cell movement using 3D time-lapse microscopy images.

We presented a deep reinforcement learning approach within an agent-based modeling system to characterize cell movement in the embryonic development of *C. elegans*. We tested our model through two scenarios within real developmental processes: *the anterior movement of the C<sub>paaa</sub> cell via intercalation and the restoration of the superficial left-right symmetry*. Our modeling system overcame the local optimization problems encountered by traditional rule-based, agent-based modeling by using greedy algorithms. It also overcame the computational challenges in the action selection which has been plagued by the traditional tabular-based reinforcement learning approach. Our system can automatically explore the cell movement path by using live microscopy images and it can provide a unique capability to model cell movement scenarios where regulatory mechanisms are not well studied. In addition, our system can be used to explore potential paths of a cell under different regulatory mechanisms or to facilitate new hypotheses for explaining certain cell movement behaviors.

## I. INTRODUCTION

Recent developments in cutting-edge live microscopy and image analysis provide a unique opportunity to systematically investigate individual cell's dynamics and quantify cellular behavior over extended period of time. Systematic single-cell analysis of *C. elegans* has led to the highly desired quantitative measurement of cellular behaviors and unprecedented opportunities [1], [2], [3]. Based on 3D time-lapse imaging, the entire cell lineage can be automatically traced, and quantitative measurements can be made on every cell to characterize its developmental behavior [4], [5], [6], [7]. These massive recordings, which contains hundreds to thousands of cells over hours to days of development, provide

<sup>1</sup>Zi Wang, Dali Wang, Chengcheng Li and Husheng Li are with the Department of Electrical Engineering and Computer Science, University of Tennessee, Knoxville, TN 37934, USA. {zwang84,dwang7,cli42,hl31}@utk.edu.

<sup>2</sup>Yichi Xu and Zhirong Bao are with the Developmental Biology Program, Sloan-Kettering Institute, New York, NY 10065, USA. {xuy2,baoz}@mskcc.org.

<sup>3</sup>Dali Wang is also with the Environmental Science Division, Oak Ridge National Laboratory, Oak Ridge, TN 37831, USA.

\*Dali Wang and Zhirong Bao are the corresponding authors.

a unique opportunity for cellular-level systems behavior recognition as well as simulation-based hypothesis testing.

Agent-based modeling (ABM) is a powerful approach to analyze complex tissues and development [8], [9], [10]. In our previous effort, an observation-driven, agent-based modeling and analysis framework was developed to incorporate large amounts of observational/phenomenological data to model the individual cell behaviors with straightforward interpolations from 3D time-lapse images [11], [12]. With the ultimate goal being to model individual cell behaviors with regulatory mechanisms, there are still tremendous challenges remain to dealing with the scenarios where regulatory mechanisms lag in data collection and potential mechanistic insights need to be examined against complex phenomena.

This paper presents a new method to model cellular movement using time-lapse images and deep neural networks within an agent-based modeling framework. Directional cell locomotion is critical in many physiological processes during *C. elegans* development, including morphogenesis, structure restoration, and nervous system formation. It is known that, in these processes, cell movements can be guided by gradients of various chemical signals, physical interactions at the cell-substrate interface and other mechanisms [13], [14], [15]. To overcome the barriers of system complexity and computational efficiency in the early stage of *C. elegans* development, where the regulation mechanisms are not well studied, deep neural networks can be adopted to characterize the movement of individual cells within an embryonic system from 3D time-lapse images directly. Specifically, deep reinforcement learning [16] methods can be used to learn and to represent individual cell movement paths under a collection of biological regulation mechanisms within a dynamic environment in the early phase of the embryonic development of *C. elegans*.

## II. MODELING APPROACH

In our modeling framework, an individual cell is modeled as an agent that contains a variety of information on its fate, size, division time, and group information. For a wild-type *C. elegans* simulation, the cell fate and division information can be directly derived from predefined observation datasets. For more complicated cases that involve gene mutation and manipulation, the developmental landscape can be incorporated for modeling purpose [3]. More detailed design information on the agent-based model can be found in [11]. In this study, the cellular movements are treated as results of inherited and genetically controlled behavior regulated by

inter- or intracellular signals, and these cell movements are also constricted by the neighbor cells and the eggshell.

We further assume that movement path of an individual cell is an optimal path that a cell can use to migrate under a collection of regulation networks and/or constraints within a physical environment. Then we can transform the cell movement problem into a neural network construction and learning problem using observation and predefined rules. Therefore, neural networks can be constructed inside each cell to represent its behavior, and the reinforcement learning method can be used to train the neural networks from 3D time-lapse imaging (with information on locations of cells, their neighbor list, and other cell interactions). After training, these neural networks can determine a feasible and optimal cell movement path in a dynamic embryonic system, but the migration path is still controlled and strained by the underlying regulation networks and physical environment.

While the regulation networks can be defined at cellular, group, tissue, or even embryonic levels, only the individual cell movement and group movement are examined and modeled in this study.

#### A. Individual Cell Movements

Two basic kinds of individual cell movements are investigated. The first movement pattern is directional movement, in which the regulation network presents strong signals (such as planar cell polarity or cell-cell adhesion [17]) and results in directional individual cell movements. The second type of cell movement, defined as passive cell movement, represents the scenarios in which no explicit movement patterns are observed when the signals from regulation networks are weak or canceled out.

1) *Directional cell movement*: At this stage, with strong regulation signals from regulation networks, cell movement is mainly controlled by the potential destination and physical pressures from neighbor cells. The destination of cell movement can be defined as a spatial location or region within the embryonic system when regulatory mechanisms are not well studied, or it can be defined as a location next to a specific cell.

2) *Passive cell movement*: At this stage, without strong overall regulation mechanisms, cell movement is mainly controlled by the physical pressures between neighbor cells or the eggshell. Therefore, it is defined as passive cell movement with a high level of randomness.

#### B. Collective Cell Migration

In a *C. elegans* system, individual cells can also be a part of functional group with group-specific communication and regulation mechanisms. In collective cell migration, all the cell movements are directional. However, depending on the role of cell movement, the cells in collective migration can be further categorized as leading cells and following cells.

### III. METHODS

#### A. ABM Framework

An agent-based modeling platform was adopted to present fundamental cell behaviors, including cell fate, division,

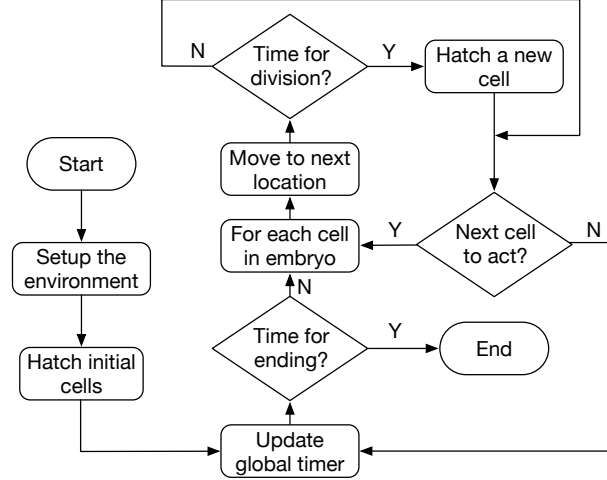


Fig. 1: ABM framework.

and migration for a wild-type *C. elegans* in which all cell fates were defined. The ABM framework, which retains two fundamental characteristics (cell movement and division) for *C. elegans* early embryogenesis is illustrated in (Fig. 1). At each time step, cells acted with either predefined behaviors (move or divide) or the output from the neural network, depending on their specific identities (dumb cells or intelligent cells). For the intelligent cell, its movement behavior was integrated in the “Move to next location” part by feeding the state into the neural network for the next moving action.

#### B. Cell Movement via Deep Q-network

As mentioned in the Modeling Approach section, cell migration has been modeled as a reinforcement learning process [18] in which certain agents (cells) interact with the environment (the whole embryo or neighbor cells) to achieve predefined goals. In an individual cell movement case, an intelligent cell always tends to seek an optimal movement path towards its destination based on the regulatory rules. At each discrete time step  $t$ , the cell senses its state  $S_t \in \mathcal{S}$  from the embryo and selects an action  $A_t \in \mathcal{A}$ , where the set of  $\mathcal{A}$  includes the candidate actions at that state. The embryo returns a numerical reward  $R_t \in \mathcal{R}$  to the cell as an evaluation of that action based on the state. Finally, the cell enters the next state  $S_{t+1}$  and repeats the process until a terminal condition is triggered. The whole process is demonstrated in Fig. 2.

Tabular-based Q-learning approaches are largely used for reinforcement learning tasks. However, a dynamic agent-based embryogenesis model usually contains hundreds of cells that act at highly temporal and spatial resolutions. Millions of different states, which are generated during a single embryogenesis process, cannot be handled by traditional tabular-based Q-learning algorithms. Recent breakthroughs in reinforcement learning that incorporate deep neural networks as mapping functions allow us to feed in high-dimension states and obtain the corresponding Q-values

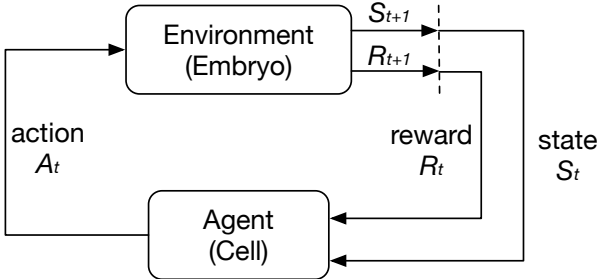


Fig. 2: Reinforcement learning framework.

[16], [19]. Such a deep Q-network (DQN) outperforms most of the previous reinforcement learning algorithms.

1) *Framework*: A deep Q-network is established based on traditional Q-learning algorithms. Rather than searching the Q-table to find the maximal value of  $Q(S_t, A_t)$ , Q-values are obtained through a neural network parametrized by a set of weights  $\theta$ . The update process (Eq. 1) can then be achieved by minimizing the loss function  $\mathcal{L}$  (Eq. 2) and back-propagating the loss through the whole neural network to update  $\theta$  by  $\theta_{t+1} = \theta_t - \alpha \nabla_{\theta} \mathcal{L}(\theta_t)$  [20].

$$Q(S_t, A_t | \theta_t) = Q(S_t, A_t | \theta_t) + \alpha \left[ R_t + \gamma \max_a Q(S_{t+1}, A_t | \theta_t) - Q(S_t, A_t | \theta_t) \right], \quad (1)$$

$$\mathcal{L}(S_t, A_t | \theta_t) = \left[ R_t + \gamma \max_a Q(S_{t+1}, A_t | \theta_t) - Q(S_t, A_t | \theta_t) \right]^2, \quad (2)$$

where  $\alpha$  is the learning rate and  $\gamma \in (0, 1)$  is the discount rate, which determines the present value of future rewards [18].

In order to improve the system's performance, we utilized two mechanisms: experience replay [16] and target network [19] in the framework. Experience replay cuts off the correlation between samples by storing the movement tuple  $(S_t, A_t, R_t, S_{t+1})$  in a replay memory and sampling them randomly during the training process. Rather than calculating the future maximal expected reward  $\max_a Q(S_{t+1}, A_t | \theta_t)$  and updating the weights in a single neural network, a target network, which has the same architecture as the original network (called the online network in the new scenario) but parameterized with  $\theta_t^-$ , was implemented for the calculation of  $\max_a Q(S_{t+1}, A_t | \theta_t^-)$ . The weights  $\theta_t^-$  remained unchanged for all  $n$  iterations until they were updated with  $\theta_t$  from the online network. The improved process is represented in Eq. 3.

$$Q(S_t, A_t | \theta_t) = Q(S_t, A_t | \theta_t) + \alpha \left[ R_t + \gamma \max_a Q(S_{t+1}, A_t | \theta_t^-) - Q(S_t, A_t | \theta_t) \right] \quad (3)$$

The neural network, which is fed with the embryo state and outputs a Q-value for each action, contained three hidden

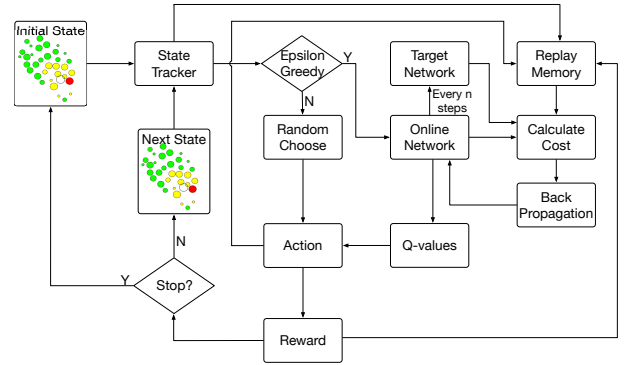


Fig. 3: Deep Q-network framework for cell movement.

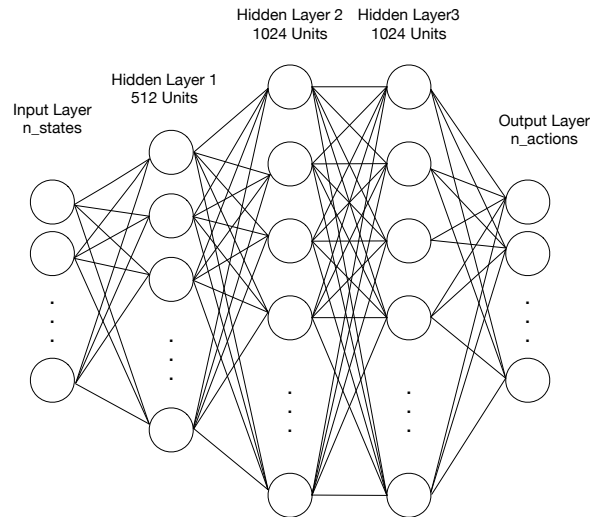


Fig. 4: Neural network architecture.

layers, with 512, 1024, and 1024 nodes, respectively (Fig. 4). The Rectified Linear Units (ReLU) was implemented as the activation function after all the hidden layers except for the output layer. The details of the hyperparameter selection can be found in the Supplementary Material S1.1.

2) *Regulatory rules and reward settings*: In the reinforcement learning scenario, the regulatory rules that guide cell movement can be translated to “rewards” as an evaluation of how well a cell moves during a certain period of time. For the constraints of the cell movements, we defined the following three rules:

- *Collision*: Cells cannot squeeze too much with each other. The closer two cells are, the larger the penalty (negative reward) they receive.
- *Boundary*: Cells cannot break through the eggshell. The closer the cell is to the eggshell, the larger the penalty (negative reward) it receives.

For both of the above rules, as a threshold of distance is reached, a termination condition is triggered. For the directional cell movement, a destination is given as a third rule when other regulatory rules are largely missing:

- *Destination*: A cell always seeks the optimal path towards its target location.

The third rule can be replaced (e.g., by following a leading cell) as regulatory mechanisms are discovered, or new hypotheses are formulated. Details of the reward setting are illustrated in Section 4 and Supplementary Material S1.2.

### C. Behavior of the Dumb Cell

Non-intelligent cells move based on live microscopy images. Because the temporal resolution of the observational data is one minute but an ABM simulation often requires a much smaller tick interval, a linear interpolation is implemented between two consecutive samples to calculate the next locations of these cells. Additionally, we added a random noise for each movement by sampling it from a normal distribution whose mean and standard deviation were averaged from the locations of the cells of 50 wild-type *C. elegans* embryos [21].

### D. Behavior of the Intelligent Cell

For the intelligent cell, an  $\epsilon$ -greedy strategy was implemented, which makes it not only act based on past experiences to maximize the accumulated rewards most of the time but also gives it a small chance to randomly explore unknown states. In the following sub-section, we give a description of the settings of the intelligent cell's input state and output action.

1) *Input states*: Representing the input state accurately and efficiently is a key issue for the deep reinforcement learning cell movement framework. Besides the location of the intelligent cell, which is indispensable, an intuitive assumption is that its neighbors, which represent the environment, should be incorporated to form the input state. We implemented a neighbor determination model [22] in a conservative manner for this purpose. Specifically, we extracted a number of candidate cells that might influence the intelligent one with a relatively loose condition, so that more cells would be selected to guarantee that the input state was sufficiently represented. This was done by running the agent-based model in a non-reinforcement learning mode and recording the candidates at each time step. Finally, we combined the locations of these cells in a fixed order as the input for the neural network.

2) *Output actions*: It is intuitive to give the intelligent cell as many candidates of action as possible so that it can make the most eligible choice during the simulation. The diversity of the action includes different speeds and directions. However, the number of output nodes grows exponentially as we take looser strategies to select the action. Based on our extensive experiments, we discovered that an enumeration of eight directions of action, with  $45^\circ$  between each of them, is good enough for this scenario. Moreover, we fixed the speed based on an estimation of the average movement speed during the embryogenesis, which was measured from the observational data.

## IV. EXPERIMENTS

### A. Computational Environment and Platform

The agent-based model was implemented with Mesa, which is an ABM framework in Python 3+. We used

Python's GUI package Tkinter for the purpose of visualization. The cell movement behavior model was built with 3D coordinates, and certain slice of the whole embryo was visualized in a 2D manner to illustrate where emergent behaviors specifically happen. We used Pytorch to achieve reinforcement learning algorithms with the advantage of GPU acceleration during the training process. The reinforcement learning architecture was integrated as part of the agent-based model. All the computations were executed in a DELL® Precision workstation, configured with a 3.6 GHz 4-core Intel® Xeon® CPU, 64 GB main memory, and a 16-GB NVIDIA® Quadro® P5000 GPU.

### B. Model Setup

Live 3D time-lapse images of *C. elegans* embryogenesis data were used to study cell movement. AceTree [23] was used to visualize observation data. Detailed information on live imaging can be found in the supplementary material S2.

Two special *C. elegans* biological phenomena, *the intercalation of Cpaaa* and *left-right asymmetry rearrangement*, were investigated. The first case is a remarkable process during *C. elegans* early morphogenesis of dorsal hypodermis. Cpaaa is born at the dorsal posterior. About 10 minutes later after its birth, Cpaaa moves towards the anterior and intercalates into two branches of ABarp cells, which will give rise to left and right seam cells, respectively. The intercalation of Cpaaa is consistent among wild-type embryos. It leads to the bifurcation of ABarp cells and the correct positioning of seam cells. The second case is *left-right asymmetry rearrangement*. It is a significant development scenario: At the 4-cell stage, the left-right symmetry is broken after the skew of ABa/ABp spindle. The right cell ABpr is positioned more posterior than the left cell ABpl. At the AB64 (64 AB cells, 88 total cells) stage, the movement of ABpl and ABpr cells start to restore the spatial symmetry, i.e., ABpl cells move towards the posterior and ABpr cells move towards the anterior. By 350-cell stage, ABpl and ABpr cells are again in symmetry on the AP axis. This asymmetry rearrangement achieves a superficially symmetric body plan [24].

For the estimation of the embryo volume, the embryo was considered to be an ellipsoid for the volume calculation. The mounting technique aligns the DV axis in the embryo with the z-axis of the data [25], and the lengths of the other two axes (AP and LR) were obtained by finding the minimum and maximum cell positions along them [21]. For the estimation of the cell radius, the ratio of the cell volume to the entire embryo was determined based on its identity. Then, the radius was calculated as we consider a cell to be a sphere [22].

We utilized linear functions to define the rewards in our simulations. Specifically, for the *Collision* rule, a penalty (negative reward) was exerted as the distance between two cells reached a threshold. As their distance became smaller, the penalty linearly grew until a terminal threshold was reached (Eq. 4). Similarly, for the *Boundary* rule, the penalty was calculated based on the distance between the intelligent cell and the eggshell. Finally, for the *Destination* rule, bigger

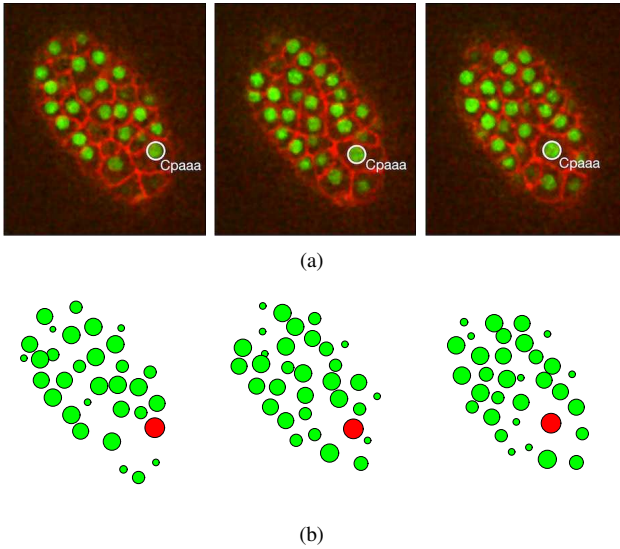


Fig. 5: Comparison between (a) the 3D time-lapse images and (b) the visualizations of the ABM simulation results.

positive rewards were given as the cell moved towards the destination.

$$r = \frac{d - d_l}{d_h - d_l} \times (r_h - r_l) + r_l, \quad (4)$$

where  $d$  is the distance between two cells and  $d_h$  and  $d_l$  represent the highest and lowest bounds of the distance between two cells where a penalty is generated.  $r_h$  and  $r_l$  indicate the range of the penalty.

### C. An Agent-based Deep Reinforcement Learning Framework for *C. elegans* Embryogenesis

The agent-based modeling environmental was initialized with the observation data from live imaging. In our first case, the ABM platform was configured to track the movements of the intercalation cell, namely, Cpaaa, for the purpose of illustration. We only considered the space that was 5-9  $\mu\text{m}$  to the dorsal side, where Cpaaa intercalation happens. The entire space was visualized by projecting it to the center plane (7  $\mu\text{m}$  to the dorsal side). Based on the result (Fig. 5) we found that the movement path of Cpaaa is consistent with that in the 3D time-lapse images. The visualized cell sizes are largely consistent with the observation data, except that a few of them, especially located in the planes far away from the center plane, hold slightly different sizes visually. However, those differences have an insignificant impact on cell movement modeling.

Unlike supervised learning tasks, such as classification and regression, evaluating the performance is quite challenging in deep reinforcement learning tasks. We followed the evaluation metric in [16] to quantify the general performance of the system. The total rewards a cell collects in a single movement path generally goes upward, but tends to be quite noisy since very tiny changes in the weights of the neural network results in large changes in the actions a cell chooses [16] (Fig. 6(a)). Training loss tends to oscillate over time

(Fig. 6(b)), and the reason behind this is the implementation of experience replay and a target network, which cuts off the correlation between training samples. Finally, we extracted a set of states by running the model in a non-reinforcement learning way and fed them to the neural network during the training process. It turns out that the average action value of these states grew smoothly during training (Fig. 6(c)). We did not encounter any divergence problems during the training process, though the convergence of DQN is still an active research area. Sometimes, we experienced a few unstable training scenarios, but this problem can be solved by implementing a learning rate decay strategy.

### D. Regulatory Mechanisms of Individual Cell Movements

We examined our hypotheses of individual cell movement in the *Cpaaa* intercalation case (see Section II-A). In this case, during the first four minutes of the process, the intercalating cell Cpaaa moved randomly. After extensive divisions of the ABarp cells, Cpaaa changed its behavior to a directional movement until the end of the process. The signal triggering the switch may have come from newborn ABarp cells.

In the directional cell movement process, unexpected regularization signals or irregular movement patterns have to be considered. In our study, we defined the possibility of choosing a directional movement from the neural network by a ratio between 0 and 1. The value of zero meant a completely random movement, and the value of one meant a completely directional cell movement.

*1) Regulatory mechanisms in the Cpaaa intercalation case:* We trained individual neural networks for directional and passive movements with different sets of regulatory mechanisms. Specifically, we trained one neural network for passive movement with the *Collision* and *Boundary* rules, and the other with the addition of the *Destination* rule. The different behaviors of Cpaaa (random movement for the first four minutes and directional movement after that) were controlled by manipulating the possibility of random movement  $\epsilon$  in the action selection procedure. Simulation results (Fig. 7(b)) show that during the first four minutes, the intelligent cell didn't have an explicit destination and, to a large extent acted randomly. After that, Cpaaa switched its behavior and began to move directionally to the destination, as well as kept proper distances from its neighbors and the eggshell. We also trained a neighbor of Cpaaa, namely, Caaaa, as a passive movement cell during the process (Fig. 7(c)). Cell movements in both scenarios largely reproduced those in the live microscopy images.

For the verification of the generality of the model, random noises were added to the initial position of all the cells (including the intelligent cells) and to all the movement paths of the dumb cells during the training process. It turns out that the neural networks can still provide the most proper actions under a large variety of input states after the policy converges, though the optimization process takes longer to converge than those in the scenarios without random noises.

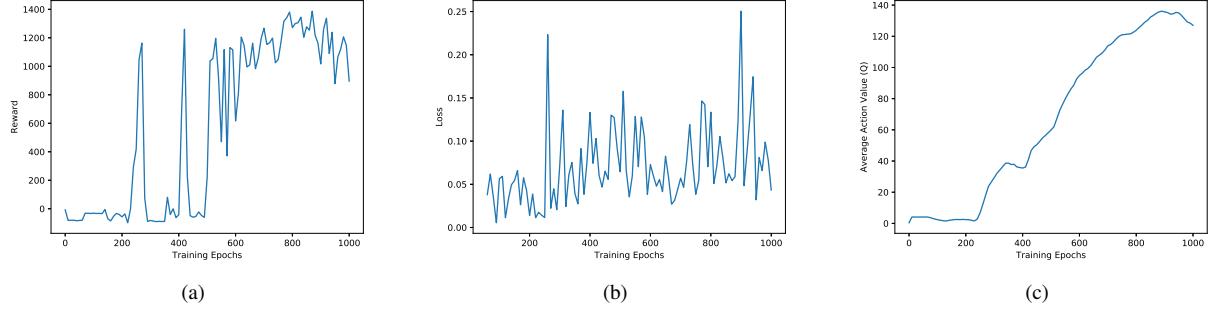


Fig. 6: The accumulated rewards, loss, and average action value over epochs.

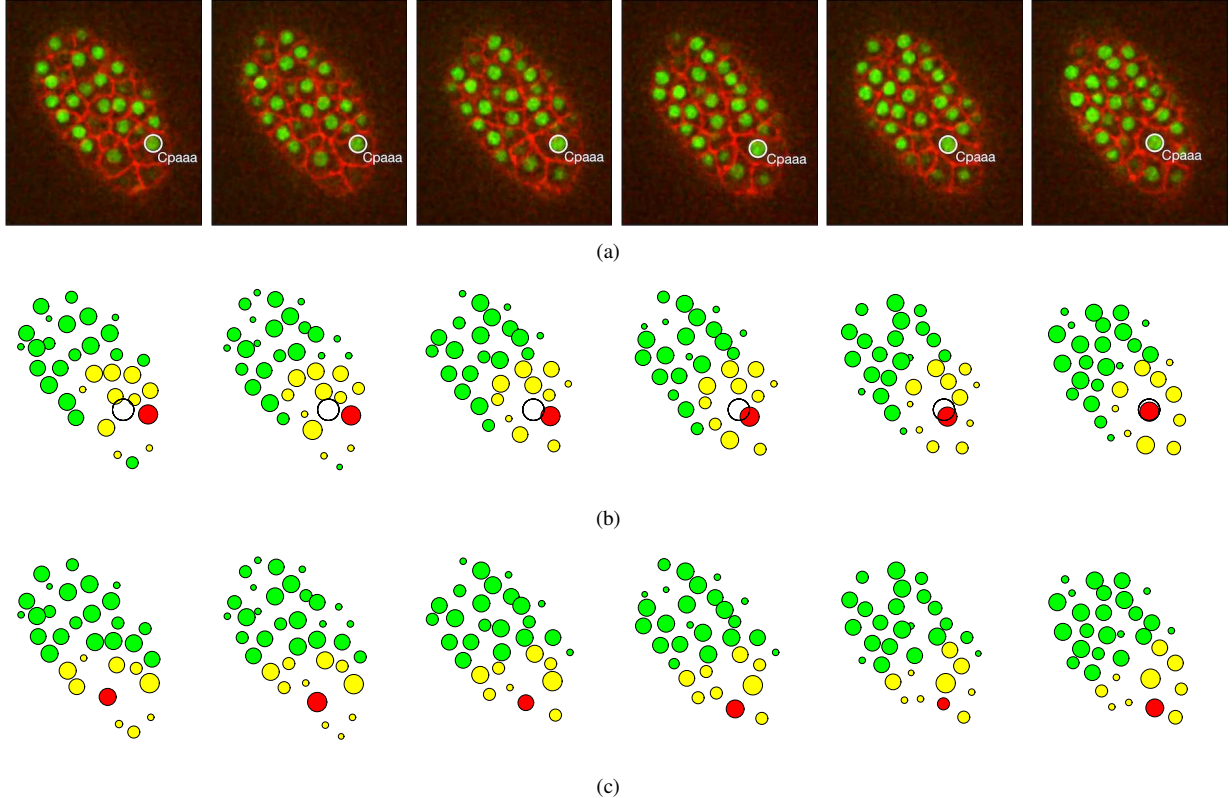


Fig. 7: Results of the *Cpaaa* intercalation case. (a) Observation results by AceTree from 3D time-lapse images. (b) Simulation results of the intercalating cell Cpaaa. (c) Simulation results of the cell Caaaa, a neighbor of Cpaaa. Red, yellow, and green circles represent the intelligent cell, input state cells, and non-related cells, respectively. The white circle indicates the destination of the intelligent cell. All three sets of data were collected at the following time steps: 0, 4, 8, 12, 17, and 22 (minutes from the beginning of the simulation).

2) *Migration path of the intelligent cell*: We found that the intelligent cell Cpaaa adopts a similar movement path to the destination, as compared to the observation case (Fig. 8), though from the 13th to 19th minute, the observation movement of Cpaaa went towards the anterior faster than the simulation path. The difference between the simulation and observation results indicates that extra regulatory mechanisms (such as cell adhesion) could be considered to control cell movement during the whole *Cpaaa* intercalation process. We have also tried experiments only with the *Boundary* and *Collision* rules. In that experiment, Cpaaa fell into a

suboptimal location where it kept proper distances with its neighbors (Fig. S3.1) and failed to identify the migration path (Fig. S3.2). Such results prove that Cpaaa's movement is not a passive movement, but strongly influenced by the *Destination* rule (or its alternatives) during the simulation. Based on the above simulations, we believe that Cpaaa's intercalation can be treated as an active cellular movement. Moreover, another interesting finding is that the standard deviation of the migration path of Cpaaa with the *Destination* rule is controlled in a proper range, whereas that of the path without the *Destination* rule diverges as time goes by. Such

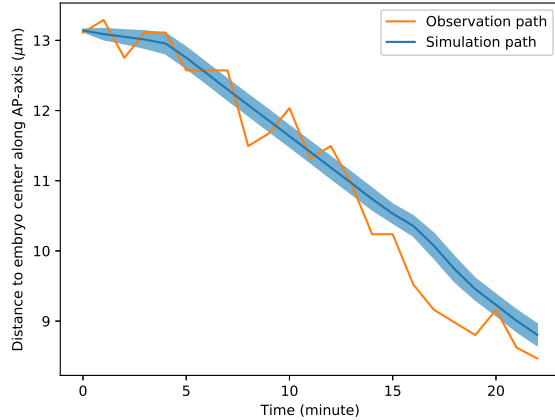


Fig. 8: Migration paths of Cpaaa. The simulation path is an average over 50 runs, and the shaded region indicates a range of one standard deviation greater/less than the average value. The horizontal axis represents the developmental time in minutes. The vertical axis represents the projected position of Cpaaa on the AP-axis to the center of the embryo.

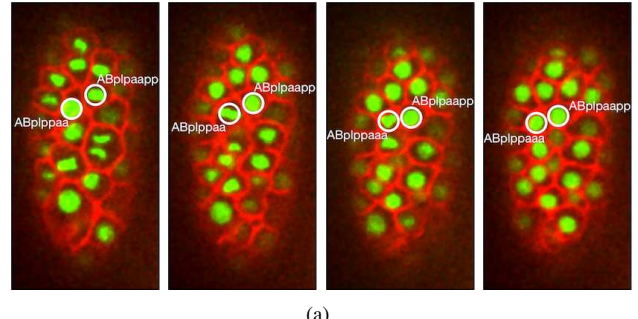
a result indicates that the intelligent cell achieves an error correction mechanism in its migration path to its destination.

#### E. Regulatory Mechanisms of Group Cell Migration

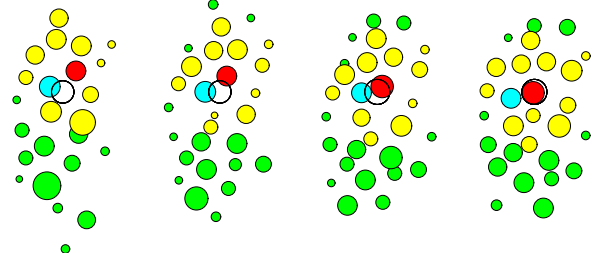
We trained another neural network to test the cell movement in group migration via the case of *left-right asymmetry rearrangement*. Rather than explicitly pointing out the destination, we let the intelligent cell (ABplpaapp) follow the leading cell (ABplppaa, or its daughter cells). The reward setting was then modified accordingly: When the distance between the leading cell and the following cell was in a proper range, a positive reward was given. The results (Fig. 9(b)) show that ABplpaapp always moves following the leading cell, and keeps proper distances from its neighbors. The results are consistent with the observation data (Fig. 9(a)), which proves the flexibility of our model by replacing the *Destination* rule with more concrete ones.

## V. DISCUSSION

In this study, we presented an approach to model cell movement using a neural network and reinforcement learning within an agent-based modeling framework. Our study showed that neural networks can be adopted to characterize cell movement and that the deep reinforcement learning approach (deep Q-network) can be used to find the optimal movement path of a cell under certain regulatory mechanisms. As comparing to the heuristic rule-based, agent-based models, with which macroscopical behaviors (such as tissue/organ morphogenesis) can be studied [8], [26], this model provides a new point of view in which single cell movements can be defined and optimized over a considerable period of time. For the situations where regulatory mechanisms lag data collection, an observed destination can be given as a dominant rule for cell movement until it is replaced by more



(a)



(b)

Fig. 9: The simulation of left-right asymmetry rearrangement. (a) Observation data. The intelligent cell and the leading cell are circled. (b) Simulation results. The cyan circle represents the leading cell, and the others are color coded, as in Fig. 7. The white circle here indicates the destination of the intelligent cell only for the purpose of visualization. Both sets of data were collected at the following time steps: 0, 3, 6, and 9 (minutes from the beginning of the simulation).

explicit, biologically driven rules. Such an approach can be utilized to test certain regulatory mechanisms or hypotheses by manipulating the rewards in the deep reinforcement learning framework and comparing simulation results with observation datasets. Moreover, by comparing the paths of the simulation and observation cases, biologists can investigate whether there are extra regulation mechanisms that control multiple segments over a long period of cell movement.

This model captures the main aspects of cell movement and provides a new idea that represents cell behaviors with neural networks trained by deep reinforcement learning algorithms. More powerful models can be implemented in the following aspects: (1) Multi-agent reinforcement learning [27], [28] can be used for studying cooperative/ competitive cell behaviors by manipulating the rewards in the framework. Such an extension can provide further biological insights. For example, for the *Cpaaa intercalation* case, we may investigate whether the certain group of cells (i.e., Cpaaa and its neighbors) works cooperatively (as a result of the intercalation of Cpaaa) or its neighbors actually act competitively with their own rules (but the regulatory rule of Cpaaa is over-dominant). (2) The hierarchical regulatory mechanism is another area of interest. As presented in [19], the deep Q-network performs poorly on such hierarchical tasks. Such tasks require more advanced strategies that are obtained by

prior knowledge, which can hardly be represented by the input state. Therefore, future work is immediately needed to implement hierarchical deep reinforcement learning architectures to meet such demand [29].

## VI. CONCLUSION

In this paper, deep reinforcement learning was used to model cell movement within an agent-based modeling framework. We showed that complex cell behaviors (i.e., cell movement in this study), as a result of the interactions between cells and their environments, can be represented by a neural network and can be trained via a deep reinforcement learning algorithm. This model can be utilized to explore potential paths of a cell movement under different regulatory mechanisms, and to explain certain cell behaviors by proposing new hypotheses on regulation networks.

## FUNDING

This study is supported by an NIH research project grants (R01GM097576). Research in the Bao lab is also supported by an NIH center grant to MSKCC (P30CA008748).

## REFERENCES

- [1] John Isaac Murray, Thomas J Boyle, Elicia Preston, Dionne Vafeados, Barbara Mericle, Peter Weisdepp, Zhongying Zhao, Zhirong Bao, Max Boeck, and Robert H Waterston, "Multidimensional regulation of gene expression in the *c. elegans* embryo," *Genome research*, vol. 22, no. 7, pp. 1282–1294, 2012.
- [2] Zhuo Du, Anthony Santella, Fei He, Michael Tiongson, and Zhirong Bao, "De novo inference of systems-level mechanistic models of development from live-imaging-based phenotype analysis," *Cell*, vol. 156, no. 1, pp. 359–372, 2014.
- [3] Zhuo Du, Anthony Santella, Fei He, Pavak K Shah, Yuko Kamikawa, and Zhirong Bao, "The regulatory landscape of lineage differentiation in a metazoan embryo," *Developmental cell*, vol. 34, no. 5, pp. 592–607, 2015.
- [4] Ralf Schnabel, Harald Hutter, Don Moerman, and Heinke Schnabel, "Assessing normal embryogenesis in *caenorhabditis elegans* using a 4d microscope: Variability of development and regional specification," *Developmental biology*, vol. 184, no. 2, pp. 234–265, 1997.
- [5] Jürgen Hench, Johan Henriksson, Martin Lüppert, and Thomas R Bürglin, "Spatio-temporal reference model of *caenorhabditis elegans* embryogenesis with cell contact maps," *Developmental biology*, vol. 333, no. 1, pp. 1–13, 2009.
- [6] Claudiu A Giurumescu, Sukryool Kang, Thomas A Planchon, Eric Betzig, Joshua Bloomkatz, Deborah Yelon, Pamela Cosman, and Andrew D Chisholm, "Quantitative semi-automated analysis of morphogenesis with single-cell resolution in complex embryos," *Development*, vol. 139, no. 22, pp. 4271–4279, 2012.
- [7] Koji Kyoda, Eru Adachi, Eriko Masuda, Yoko Nagai, Yoko Suzuki, Taeko Oguro, Mitsuru Urai, Ryoko Arai, Mari Furukawa, Kumiko Shimada, et al., "Wddd: worm developmental dynamics database," *Nucleic acids research*, vol. 41, no. D1, pp. D732–D737, 2012.
- [8] Yaki Setty, "Multi-scale computational modeling of developmental biology," *Bioinformatics*, vol. 28, no. 15, pp. 2022–2028, 2012.
- [9] Andy L Olivares, Miguel A González Ballester, and Jérôme Noailly, "Virtual exploration of early stage atherosclerosis," *Bioinformatics*, vol. 32, no. 24, pp. 3798–3806, 2016.
- [10] Stefan Hoehme and Dirk Drasdo, "A cell-based simulation software for multi-cellular systems," *Bioinformatics*, vol. 26, no. 20, pp. 2641–2642, 2010.
- [11] Zi Wang, Benjamin J Ramsey, Dali Wang, Kwai Wong, Husheng Li, Eric Wang, and Zhirong Bao, "An observation-driven agent-based modeling and analysis framework for *c. elegans* embryogenesis," *Plos one*, vol. 11, no. 11, pp. e0166551, 2016.
- [12] Eric Wang, Anthony Santella, Zi Wang, Dali Wang, and Zhirong Bao, "Visualization of 3-dimensional vectors in a dynamic embryonic systemwormguides," *Journal of Computer and Communications*, vol. 5, no. 12, pp. 70, 2017.
- [13] Jen-Yi Lee and Bob Goldstein, "Mechanisms of cell positioning during *c. elegans* gastrulation," *Development*, vol. 130, no. 2, pp. 307–320, 2003.
- [14] David Shook and Ray Keller, "Mechanisms, mechanics and function of epithelial–mesenchymal transitions in early development," *Mechanisms of development*, vol. 120, no. 11, pp. 1351–1383, 2003.
- [15] Chun-Min Lo, Hong-Bei Wang, Micah Dembo, and Yu-li Wang, "Cell movement is guided by the rigidity of the substrate," *Biophysical journal*, vol. 79, no. 1, pp. 144–152, 2000.
- [16] Volodymyr Mnih, Koray Kavukcuoglu, David Silver, Alex Graves, Ioannis Antonoglou, Daan Wierstra, and Martin Riedmiller, "Playing atari with deep reinforcement learning," *arXiv preprint arXiv:1312.5602*, 2013.
- [17] Carl-Philipp Heisenberg and Yohanns Bellaïche, "Forces in tissue morphogenesis and patterning," *Cell*, vol. 153, no. 5, pp. 948–962, 2013.
- [18] Richard S Sutton and Andrew G Barto, *Reinforcement learning: An introduction*, vol. 1, MIT press Cambridge, 1998.
- [19] Volodymyr Mnih, Koray Kavukcuoglu, David Silver, Andrei A Rusu, Joel Veness, Marc G Bellemare, Alex Graves, Martin Riedmiller, Andreas K Fidjeland, Georg Ostrovski, et al., "Human-level control through deep reinforcement learning," *Nature*, vol. 518, no. 7540, pp. 529–533, 2015.
- [20] Maxim Egorov, "Multi-agent deep reinforcement learning," 2016.
- [21] Julia L Moore, Zhuo Du, and Zhirong Bao, "Systematic quantification of developmental phenotypes at single-cell resolution during embryogenesis," *Development*, vol. 140, no. 15, pp. 3266–3274, 2013.
- [22] Zi Wang, Dali Wang, Husheng Li, and Zhirong Bao, "Cell neighbor determination in the metazoan embryo system," in *Proceedings of the 8th ACM International Conference on Bioinformatics, Computational Biology, and Health Informatics*. ACM, 2017, pp. 305–312.
- [23] Thomas J Boyle, Zhirong Bao, John I Murray, Carlos L Araya, and Robert H Waterston, "Acetree: a tool for visual analysis of *caenorhabditis elegans* embryogenesis," *BMC bioinformatics*, vol. 7, no. 1, pp. 275, 2006.
- [24] Christian Pohl and Zhirong Bao, "Chiral forces organize left-right patterning in *c. elegans* by uncoupling midline and anteroposterior axis," *Developmental cell*, vol. 19, no. 3, pp. 402–412, 2010.
- [25] Zhirong Bao, John I Murray, Thomas Boyle, Siew Loon Ooi, Matthew J Sandel, and Robert H Waterston, "Automated cell lineage tracing in *caenorhabditis elegans*," *Proceedings of the National Academy of Sciences of the United States of America*, vol. 103, no. 8, pp. 2707–2712, 2006.
- [26] Yaki Setty, Irun R Cohen, Yuval Dor, and David Harel, "Four-dimensional realistic modeling of pancreatic organogenesis," *Proceedings of the National Academy of Sciences*, vol. 105, no. 51, pp. 20374–20379, 2008.
- [27] Lucian Busoni, Robert Babuska, and Bart De Schutter, "A comprehensive survey of multiagent reinforcement learning," *IEEE Transactions on Systems, Man, And Cybernetics-Part C: Applications and Reviews*, 38 (2), 2008, 2008.
- [28] Ardi Tampuu, Tambet Matiisen, Dorian Kodelja, Ilya Kuzovkin, Kristjan Korjus, Juhan Aru, Jaan Aru, and Raul Vicente, "Multiagent cooperation and competition with deep reinforcement learning," *Plos one*, vol. 12, no. 4, pp. e0172395, 2017.
- [29] Tejas D Kulkarni, Karthik Narasimhan, Ardavan Saeedi, and Josh Tenenbaum, "Hierarchical deep reinforcement learning: Integrating temporal abstraction and intrinsic motivation," in *Advances in Neural Information Processing Systems*, 2016, pp. 3675–3683.